

Supplementary Table 1. Patient characteristics

#	Gender (F/M)	Age (yrs)	HR (bpm)	Disease
1	F	39	72	Hypertrophic cardiomyopathy
2	M	64	55	Mild mitral and tricuspid regurgitation
3	F	74	80	Normal
4	F	62	61	Myocardial infarction
5	M	39	65	Mitral regurgitation
6	M	67	65	Non-ischemic cardiomyopathy
7	M	59	56	Normal
8	M	68	68	Mitral regurgitation
9	M	62	69	Mitral regurgitation
10	F	32	68	Mild mitral regurgitation
11	M	69	50	Cardiomyopathy
12	F	30	63	Mild mitral regurgitation
13	F	22	74	Mild mitral and tricuspid regurgitation
14	M	63	55	Mitral and tricuspid regurgitation
15	M	75	73	Mitral regurgitation
16	M	55	55	Mitral regurgitation
17	M	31	65	Normal
18	F	63	54	Mild mitral and tricuspid regurgitation
19	M	60	53	Mild mitral and tricuspid regurgitation
20	M	64	58	Mild mitral regurgitation
21	F	71	69	Mild aortic and mitral regurgitation
22	F	72	55	Aortic stenosis, mild mitral and aortic regurgitation
23	F	43	75	Normal
24	F	77	55	Biatrial enlargement
25	M	71	66	Hypertrophic cardiomyopathy
26	F	58	54	Non-obstructive hypertrophic cardiomyopathy
27	M	73	51	Hypertrophic cardiomyopathy
28	F	64	61	Normal
29	M	45	60	Athletic cardiomyopathy
$\mu \pm \sigma$		58±16	62±8	

* F: female; M: male; HR: heart rate; μ : mean; σ : standard deviation

Supplementary Table 2. Left ventricular function and structure parameters extracted from ECG-segmented and free-breathing Real-time cine images in 29 subjects.

	ECG-segmented Cine	Real-time Cine	
		Complex-Valued-Net	Magnitude-Net
LVEF (%)	58.1±12.7	57.3±11.5	55.9±11.6
LVEDV (ml)	182.2±52.3	183.1±56.1	181.7±55.7
LVESV (ml)	77.8±37.5	80.0±36.6	81.4±37.1
LVSV (ml)	104.5±34.5	103.1±32.0	100.3±35.1
LVMass (g)	114.0±39.0	116.3±38.9	115.6±39.8

*LVEF: left-ventricular ejection fraction; LVEDV: left-ventricular end-diastolic volume; LVESV: left-ventricular end-systolic volume; LVSV: left-ventricular stroke volume; LVMass: left-ventricular mass.

Supplementary Table 3. Differences between ECG-Segmented cine and Real-time cine in quantification of left-ventricular function and structure in 29 patients

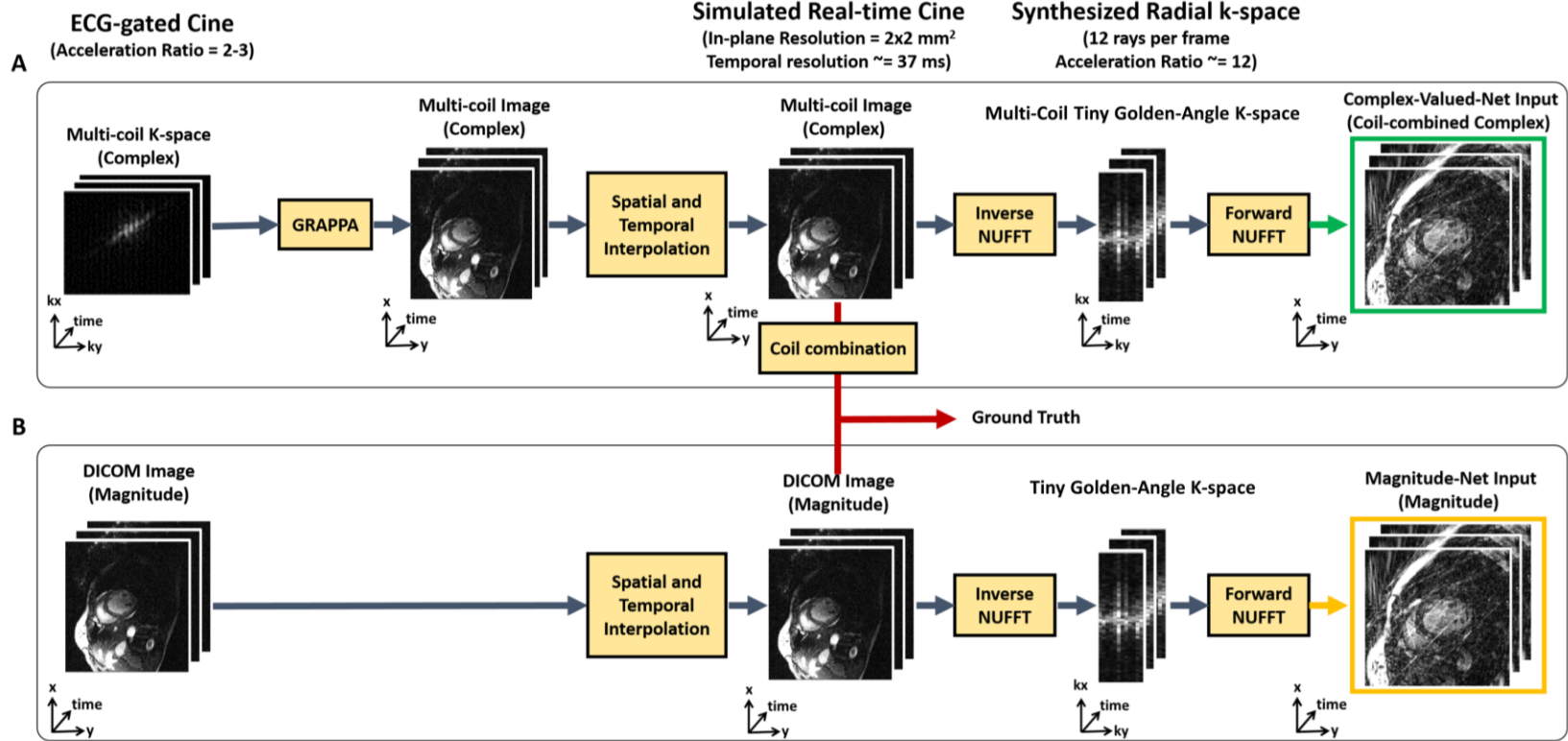
	Complex-Valued-Net vs ECG-Segmented Cine		Magnitude-Net vs ECG-Segmented Cine		Complex-Valued-Net vs Magnitude-Net	
	Mean difference (95% CI)	P	Mean difference (95% CI)	P	Mean difference (95% CI)	P
LVEF	-0.86 (-3.32, 1.60)	0.48	-2.26 (-4.19, -0.33)	0.02	1.40 (-0.53, 3.33)	0.15
LVEDV	0.86 (-4.30, 6.02)	0.73	-0.55 (-6.45, 5.35)	0.85	1.41 (-1.67, 4.49)	0.36
LVESV	2.25 (-2.49, 6.99)	0.34	3.66 (-0.08, 7.39)	0.05	-1.41 (-4.73, 1.91)	0.39
LVSV	-1.39 (-7.59, 4.81)	0.65	-4.20 (-10.07, 1.67)	0.15	2.82 (-1.77, 7.40)	0.22
LVMass	2.24 (-3.55, 8.03)	0.43	1.57 (-5.28, 8.43)	0.64	0.67 (-3.43, 4.77)	0.74

*The difference between Complex-Valued-Net/Magnitude-Net real-time cine and ECG-Segmented Cine was defined as Complex-Valued-Net/Magnitude-Net values minus ECG-Segmented Cine value. The difference between Complex-Valued-Net and Magnitude-Net was defined as Complex-Valued-Net values minus Magnitude-Net values. LVEF: left-ventricular ejection fraction; LVEDV: left-ventricular end-diastolic volume; LVESV: left-ventricular end-systolic volume; LVSV: left-ventricular stroke volume; LVMass: left-ventricular mass.

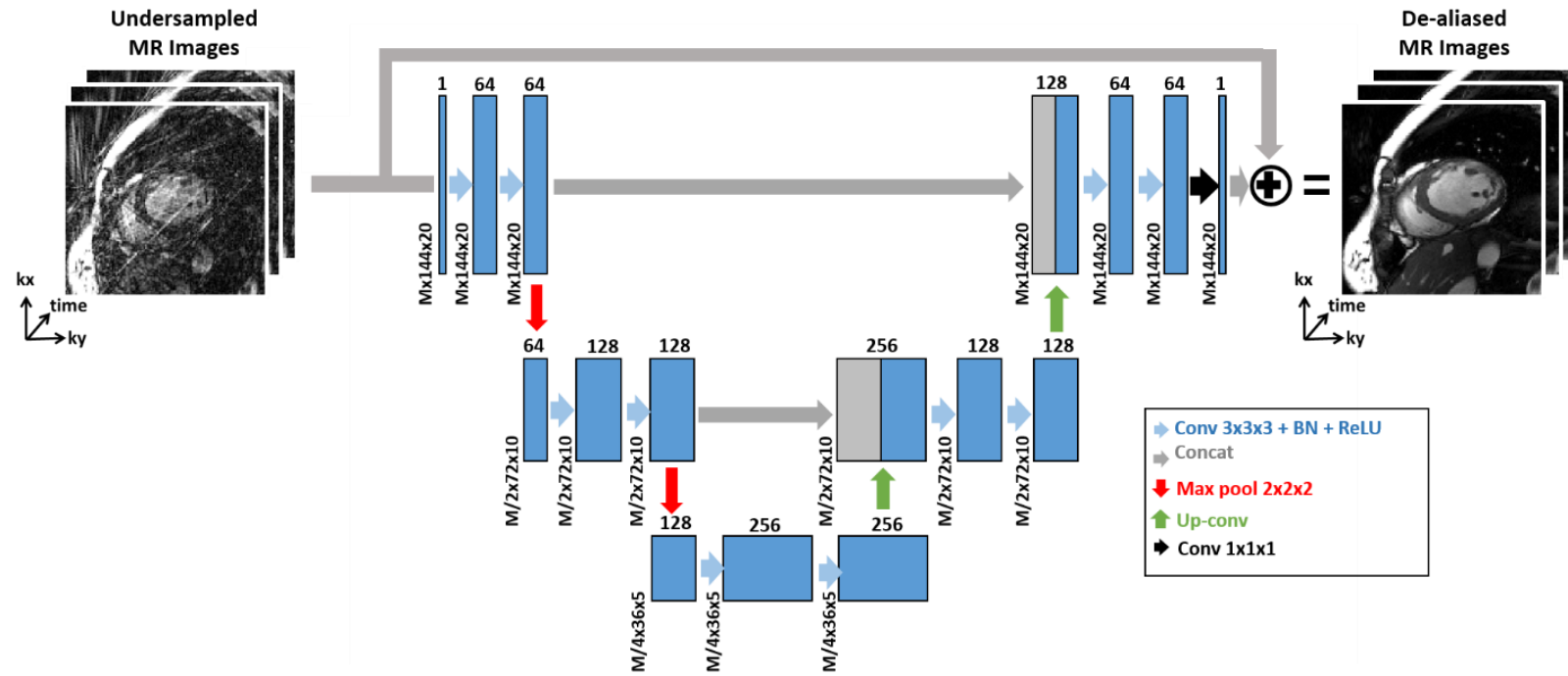
Supplementary Table 4. Percentage of two grade groups (1-3 and 4-5) of image quality scores in 29 patients

	ECG-Segmented Cine		Complex-Valued-Net		Magnitude-Net	
	1-3	4-5	1-3	4-5	1-3	4-5
Myocardial Edge	6 (21%)	23 (79%)	15 (52%)	14 (48%)	29 (100%)	0 (0%)
Temporal Fidelity	6 (21%)	23 (79%)	26 (89%)	3 (10%)	29 (100%)	0 (0%)
Artifact	7 (24%)	22 (76%)	25 (86%)	4 (14%)	29 (100%)	0 (0%)

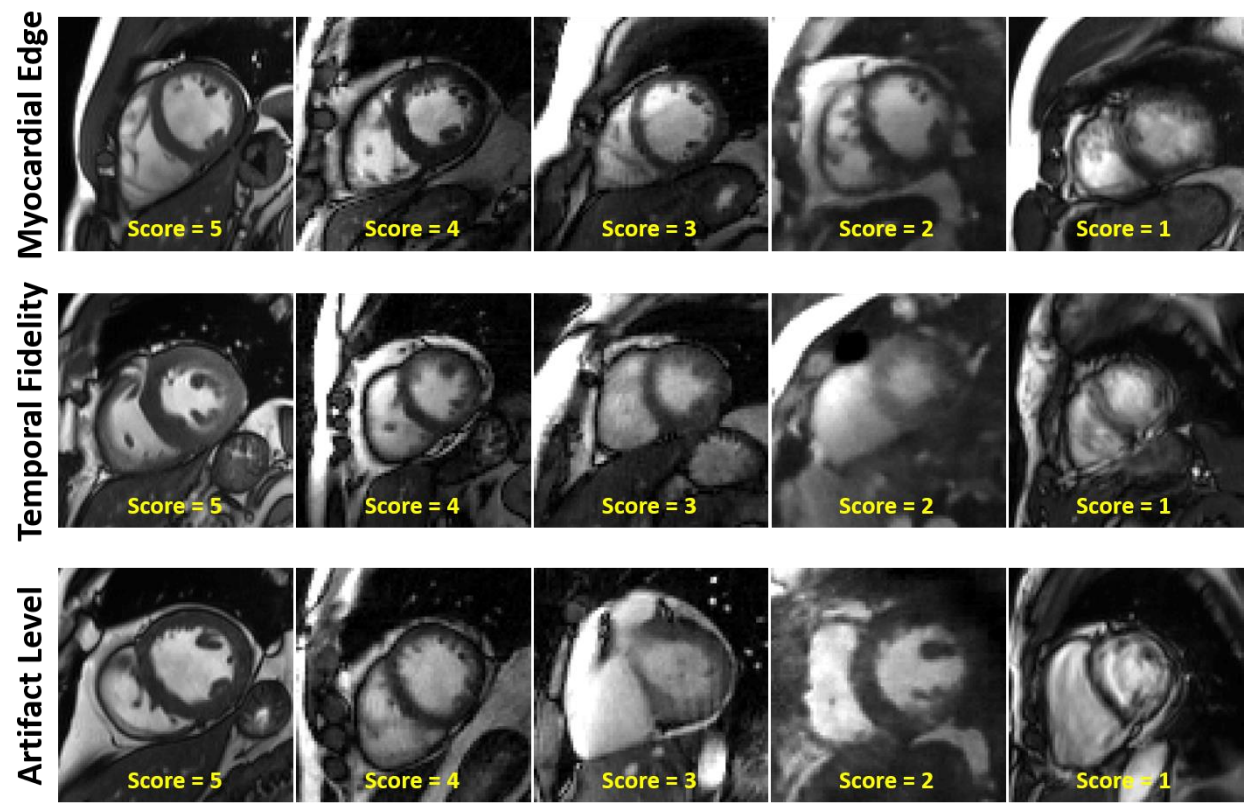
*For myocardial edge and temporal fidelity, 1: nondiagnostic; 2: poor; 3: adequate; 4: good; 5: excellent. For artifact, 1: nondiagnostic; 2: severe; 3: moderate; 4: mild; 5: minimal.



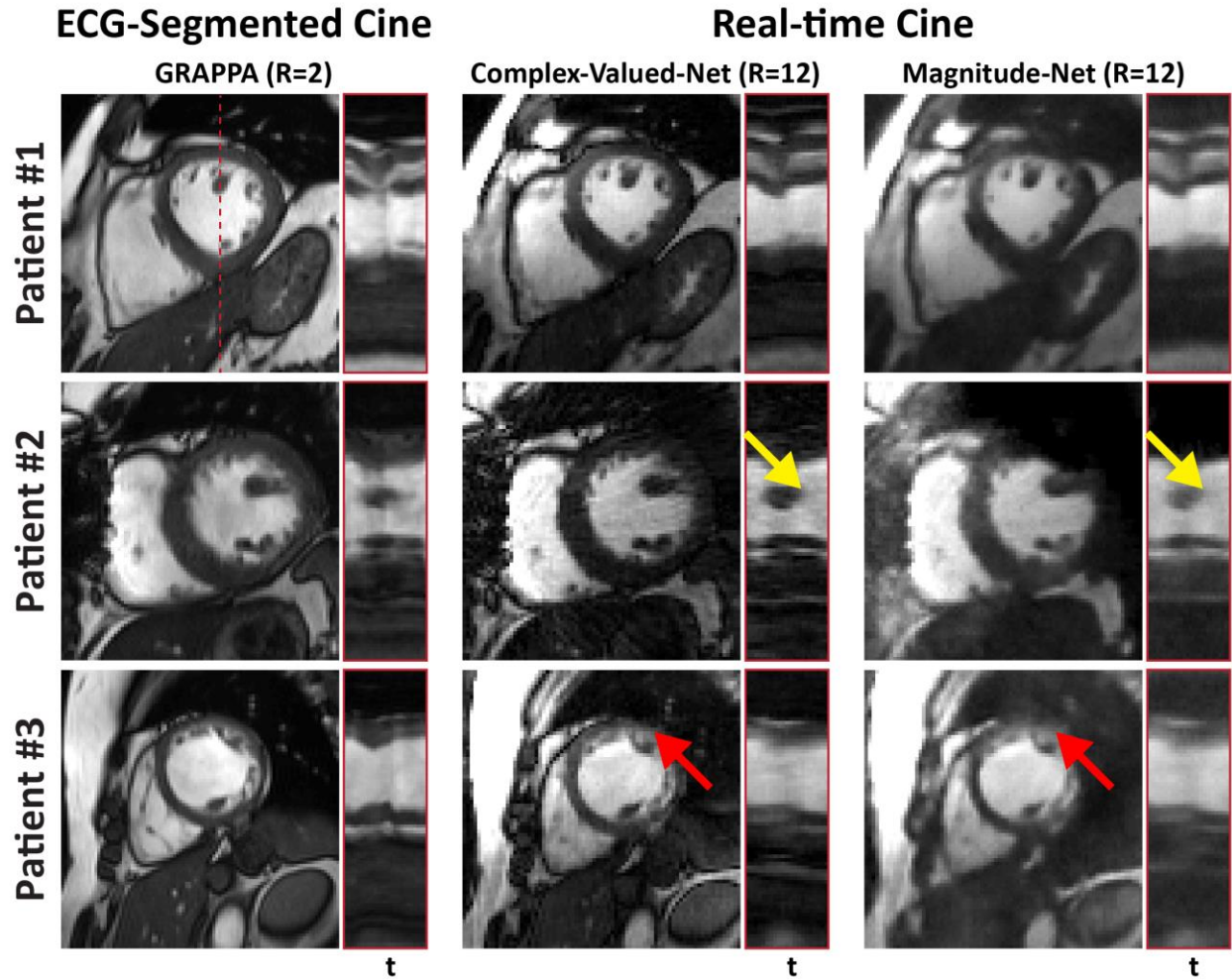
Supplementary Figure 1. Workflows processes for producing synthetic real-time cine datasets for Complex-Valued-Net and Magnitude-Net. **A.** The source images for Complex-Valued-Net are complex-valued, multi-coil k-space raw-data. GRAPPA was used to reconstruct accelerated (2-3 fold) complex-valued, multi-coil, ECG-gated segmented cine images. Spatial and temporal resolution for multi-coil images was interpolated to match prospectively acquired free-breathing real-time cine datasets. Inverse and forward NUFFT was used to produce multi-coil, complex-valued synthetic real-time cine images. Coil-combined, complex-valued synthetic real-time and ECG-gated segmented cine images were used as input/output pairs for Complex-Valued-Net. **B.** Source images for Magnitude-Net were DICOM images of ECG-gated segmented cine exported from the scanner. Spatial and temporal resolution for DICOM images were also interpolated to match prospectively acquired real-time cine datasets. Real-valued, synthetic real-time and ECG-gated segmented cine images generated using DICOM images were used as input/output pairs for Magnitude-Net.



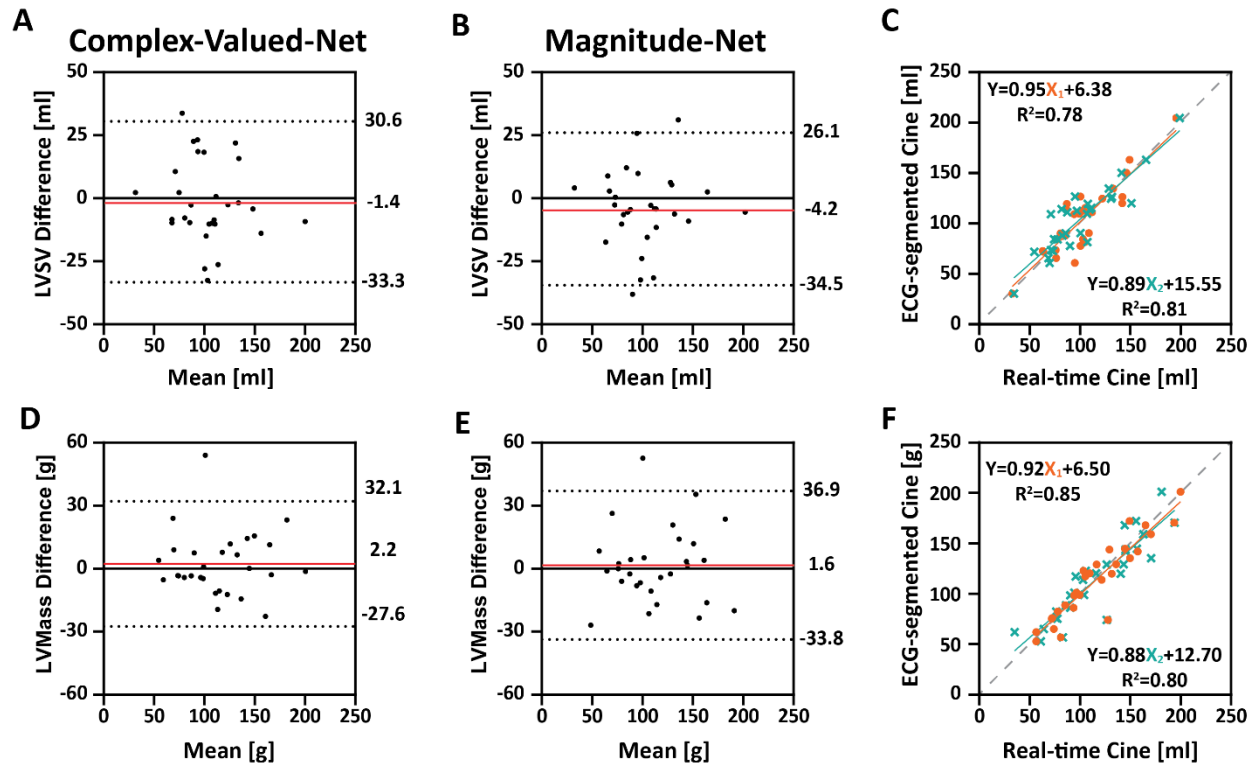
Supplementary Figure 2. Architecture of Complex-Valued-Net and Magnitude-Net using 3D U-net was composed of a set of $3 \times 3 \times 3$ convolutional kernels with batch normalization (BN) and ReLU activation, $2 \times 2 \times 2$ max pooling layers, $2 \times 2 \times 2$ convolution transpose layers, and skip connections. For Magnitude-Net, a ReLU operator was positioned at the final layer to force the output to be non-negative. M is 144 and 288 for magnitude and complex-valued inputs, respectively.



Supplementary Figure 3. Representative image for scoring criterion.



Supplementary Figure 4. Diastolic images from three patients using ECG-segmented Cartesian cine and real-time radial cine reconstructed by Complex-Valued-Net and Magnitude-Net. Images reconstructed by Complex-Valued-Net exhibit lower temporal blurring (yellow arrow) and less image artifact (red arrow) compared to those by Magnitude-Net.



Supplementary Figure 5. Comparison between ECG-segmented cine and Real-time cine using two deep learning-based reconstructions (Complex-Valued-Net and Magnitude-Net) for quantification of left-ventricular stroke volume (LVS) and left-ventricular Mass (LVMass). Bland-Altman analysis shows the agreement between real-time cine reconstructed using Complex-Valued-Net (A and B) and Magnitude-Net (D and E) with ECG-segmented cine. Dotted lines indicate upper and lower 95% limits of agreement, and the red line represents the mean difference. The difference is calculated as Real-time cine (Complex-Valued-Net and Magnitude-Net) minus ECG-Segmented cine. C-F: The corresponding linear regression (X_1 : Real-time cine by Complex-Valued-Net; X_2 : Real-time cine by Magnitude-Net). Quantification of LVS and LVMass did not differ significantly between ECG-segmented cine and free-breathing real-time cine regardless of reconstruction by Complex-valued Net or Magnitude-Net (All $P > 0.0167$).

Supplementary Video 1: Example movie of one patient acquired by breath-holding ECG-segmented cine.

Supplementary Video 2: Real-time cine reconstructed by Complex-Valued-Net from of the same subject as **Supporting Video S1**.

Supplementary Video 3: Real-time cine reconstructed by Magnitude-Net from the same subject as **Supporting Videos S1** and **S2**.

Supplementary Video 4: Real-time cine reconstructed by gridding alone from the same subject as **Supporting Videos S1, S2, and S3**.